Characterization of Frequency-Dependent Responses of the Vascular System to Repetitive Vibration

Kristine Krajnak, PhD, G. Roger Miller, BS, Stacey Waugh, MS, Claud Johnson, BS, Shengqiao Li, PhD, and Michael L. Kashon, PhD

Objective: The current frequency weighting proposed in the International Standards Organization-5349 standard may underestimate the risk of injury associated with exposure to vibration >100 Hz. The goal of this study was to assess the frequency-dependent responses of the peripheral vascular system to repeated bouts of vibration. **Methods:** The effects of exposure to vibration at 62.5, 125, or 250 Hz (constant acceleration of 49 m/s^2) on vascular morphology, oxidative stress, inflammation, and gene expression were examined in the ventral tail artery of rats. **Results:** Vascular responses indicative of dysfunction (eg, remodeling and oxidative activity) became more pronounced as the frequency of the exposure increased. **Conclusion:** Exposure to vibration frequencies that induce the greatest stress and strain on the tail (ie, >100 Hz) result in vascular changes indicative of dysfunction.

Learning Objectives

- Review basic information on hand-arm vibration syndrome, including previous knowledge of the effects of vibration exposure related to tool use.
- Summarize the methods and findings of the authors' experimental approach to assessing vascular system responses to different vibration frequencies.
- Discuss the implications of the new findings for current occupational standards for frequency exposure and the risk of vibration injury.

Approximately 1.5 million US workers are in occupations where they are regularly exposed to hand-transmitted vibration (Bureau of Labor Statistics, 2007), and based on epidemiologic studies, approximately 50% of these workers are at risk for developing hand-arm vibration syndrome (HAVS[1]). HAVS is characterized by dysfunction of the peripheral vascular and sensorineural systems. Nevertheless, the most common symptom of HAVS is cold-induced vasospasms and blanching of the digits (ie, vibration-induced white finger [VWF]; for review Ref. 2). Although a number of studies have described changes in vascular morphology[3] and sensitivity to vasodilating and vasoconstricting factors in workers with VWF,[4–6] the mechanisms by which vibration leads to these changes is unknown.

One factor that seems to affect the risk of developing VWF is the frequency of the vibration to which workers are exposed to when using tools. Experimental studies have demonstrated that the physical (ie, biodynamic) response of the human hand-arm system is frequency dependent.[7,8] The resonant frequency of the hand-arm system as a complete unit is between 16 and 62.5 Hz. However, the resonant frequency of the fingers alone is in the range of 150 to 300 Hz, and vibration at frequencies greater than 100 Hz is completely absorbed by the tissues of the fingers and hands and is not transmitted to the rest of the hand-arm system.[9,10] Absorption of these higher frequency vibrations by the tissues of the fingers and hands may result in greater shear and bending stresses in the local soft tissues, and it has been hypothesized that the increase in tissue stress and strain induced by these exposures may increase the risk of injury.[11] However, the International Standards Organization (ISO) standard 5349-1 and American National Standards Institute (ANSI) standard 2.70 assign greater weight to lower frequency vibration exposures (ie, <32.5 Hz) and less weight to higher frequency (>100 Hz) exposures, indicating that lower frequency exposures generate a greater risk of injury. Thus, the standards may underestimate the risk of injury to the fingers and hands associated with exposure to higher frequency vibration. To improve the standards and reduce the incidence of VWF, it is critical to determine how vibration frequency affects the risk of developing vascular dysfunction.

The goal of this study was to determine if adverse vascular responses to vibration are frequency dependent using a rat-tail model that we developed to assess the effects of vibration on vascular and sensorineural function.[12–14] We previously characterized the biodynamic response of the tail to vibration of different frequencies and amplitudes and demonstrated that the resonant frequencies of the tail are between 150 and 300 Hz, depending on the precise location of measurement along the length of the tail.[15] We also found that vibration transmissibility to the tail (ie, the magnitude of tail displacement/the magnitude of vibration platform displacement) was frequency dependent, with transmissibility being nearly 1 at 62.5 Hz, and gradually increasing with increases in frequency up to about 250 Hz. Thus, the physical response of the tail to vibration is similar to the response of the human fingers, especially within the frequency range that may pose the greatest risk for inducing vascular injury.

Vascular responses to vibration have been assessed after acute exposures in rats. These studies have found that vibration induces increases in oxidative activity in ventral tail and paw arteries of rats[14,16,17] and an increased sensitivity to α2C-adrenoreceptor-mediated vasoconstriction.[12] Longer exposures to vibration also result in an increase in oxidative activity, an increased sensitivity to α2C-mediated vasoconstriction, and a reduction in endothelial-mediated vasodilation.[14] These changes in responsiveness to vasomodulating factors and oxidative activity could result in vascular remodeling, characterized by a reduction in the diameter of the lumen, an increase in the thickness of the vascular smooth

From the Engineering and Controls Technology Branch (Dr Krajnak, Dr Miller, Dr Waugh, Dr Johnson), and Biostatics and Epidemiology Branch (Dr Li, Dr Kashon), National Institute for Occupational Safety and Health, Health Effects Laboratory Division, Morgantown, WVa.

Kristine Krajnak, Roger Miller, Claud Johnson, and Shengqiao Li have no financial interest in this research.

The JOEM Editorial Board and planners have no financial interest related to this research.

Address correspondence to: Kristine Krajnak, PhD, Biostatics and Epidemiology Branch, NIOSH, 1095 Willowdale Road, MS2027, Morgantown, WV 26505; E-mail: ksk1@cdc.gov.

DOI: 10.1097/JOM.0b013e3181e12b1f

muscle (VSM),[18,19] and more permanent changes in vascular function. In addition, vibration-induced vascular injury could also result in inflammation, which is also capable of inducing remodeling.[20,21] Based on these data, we used our rat-tail model of vibration to test the hypothesis that vibration frequencies that induce the greatest biodynamic response and tissue stress will result in greater increases in oxidative activity, inflammation, and vascular remodeling. To begin to identify other cellular pathways that contribute to vibration-induced changes in vascular function and remodeling, we also used total rat genome arrays and quantitative polymerase chain reaction (PCR) to assess transcriptome responses in rats exposed to different vibration frequencies.

MATERIALS AND METHODS

Animals

Male Sprague-Dawley (Hla: SD CVF rats; aged 6 weeks at arrival; Hilltop Lab Animals, Inc, Scottdale, PA; body weights 310 to 320 g [±3.2 g]) were used in this study. Rats were maintained in a colony room with a 12:12 reversed light:dark cycle (lights off 7 AM) with Teklad 2918 rodent diet and tap water available ad libitum, at the National Institute for Occupational Safety and Health (NIOSH) facility, which is accredited by the Association for Assessment and Accreditation of Laboratory Animal Care International. Rats were allowed to acclimate to the laboratory for 1 week before beginning the study. All procedures were approved by the NIOSH Animal Care and Use Committee and were in compliance with the Public Health Service Policy on Humane Care and Use of Laboratory Animals and the NIH Guide for the Care and Use of Laboratory Animals.

Vibration Exposures

The equipment and protocol for exposing animals to vibration has been previously described.[12] Briefly, rats were placed in Broome style restrainers for 1 to 2 hours a day for 5 days to acclimate them to the restrainer. After a week of acclimation to restraint, rats were randomly assigned to a cage-control group, restraint-control group, or one of three vibration groups, where vibration exposure frequencies were 62.5, 125, or 250 Hz, respectively. During exposures, vibrated rats had their tails secured to a vibrating platform. Restraint-control rats were placed in the chambers along with vibrated rats, but their tails were strapped to platforms that were mounted on isolation blocks, and cage-control rats were maintained in the colony room. Each exposure was performed between 9 AM and 1 PM and was 4 hours in length. Rats were exposed to vibration or restraint for 10 consecutive days. After each exposure, rats were returned to their home cages and housed in the colony room. The acceleration used for all vibration frequencies was 49 m/s^2 root mean squared (unweighted acceleration). The accelerations used in this study are similar to the unweighted accelerations that a worker would be exposed to if using a riveter (62.5 Hz), a sander, or a grinder (125 to 250 Hz). We also chose to test these frequencies because we have demonstrated that vibration transmissibility was different at these frequencies and thus we can use these exposures to determine how frequency-dependent changes in stress and strain affect injury.[15]

Tissue Samples

One hour after the final exposure, rats were deeply anesthetized using pentobarbital (100 mg/kg) and exsanguinated by cardiac puncture. We chose this time point, because, in the human fingers, vibration can result in a reduction in blood flow that lasts at least 45 minutes after vibration in subjects exposed to frequencies above 100 Hz.[22] In addition, animal studies have demonstrated that vibration results in a vasoconstriction that is apparent for at least 1 hour after completion of the exposure.[23] Ventral tail arteries were dissected from the C9 to C10 and C15 to C18 regions of the tail. These segments were chosen because the biodynamic response to vibration is frequency dependent in these regions of the tail and shows different responses to the three exposure frequencies.[15] The C9 to C10 region of the ventral tail artery was immediately dissected from the tail, placed into a cryovial, frozen in liquid nitrogen, and stored at −80°C until RNA was isolated. The ventral tail artery also was dissected from the C15 to C16 segment of the tail, embedded in a piece of liver tissue, frozen on dry ice, and stored at −80°C until it was sectioned for immunohistochemistry (IHC). The C17 to C18 segments of each rat's tail were placed in 15-mL conical tubes and immersion fixed overnight using 4% paraformaldehyde + 0.1 M phosphate buffer, pH 7.3. In previous studies, we have demonstrated that vibration-induced increases in oxidative activity and changes in responsiveness to adrenoreceptor-mediated vasoconstriction and acetylcholine-induced vasodilation are similar in these regions of the tail.[14] The next morning, the ventral-tail artery was dissected from the fixed segment and placed in 2-mL cryovials containing 1.5 mL of 10 mM phosphate buffered saline. Vials were stored at 4°C until processed for morphological analyses.

Morphology

Fixed artery samples were dehydrated at room temperature with agitation using increasing concentrations of ethanol. Dehydrated samples were embedded using a JB4 Embedding Kit (Electron Microscopy Sciences, Hatfield, PA) following manufacturers instructions. Briefly, samples were incubated in JB4 Infiltration solution at 4°C overnight with agitation. The next morning fresh solution was added, and after 4 hours of incubation, arteries were removed and placed in 2 × 15 × 5-mm molding trays (Electron Microscopy Sciences). Embedding solution (1.2 mL) was added to each mold. Samples were allowed to polymerize on the bench at room temperature overnight.

Artery cross-sections, 4-μm thick, were cut using a Sorvall JB-4 Microtome (DuPont Instruments, Newton, CT). Sections were wet mounted on microscope slides and dried at 60°C for 5 minutes. Arteries were stained using Lee's methylene blue, dehydrated in 95% ethanol, dried, and coverslipped with Permount (Fisher, Pittsburgh, PA). Images of arteries were captured on an AX70 Olympus microscope using a 20× air objective and a 2000R Retiga color camera. Images were imported into Scion Image (Scion, Inc, Frederick, MD), the perimeter of each lumen and of the whole artery was measured, and the diameter was calculated. VSM thickness was also measured at four points around the artery; the first measurement was made at the top of the artery and the next three measurements were made at 90-degree intervals from the previous measurement. An average thickness was calculated from the four measures and used for analyses.

Illumina Rat Expression Arrays

RNA was isolated and purified using the RNeasy Fibrous Tissue Mini Kit (Qiagen Sciences, Valencia, CA). RNA concentrations were determined using a ND-1000 UV/Vis spectrophotometer (NanoDrop Technologies, Wilmington, DE). Purity and integrity of the RNA were measured using the Agilent 2100 bioanalyzer and an RNA LabChip Kit (Agilent Technologies, Santa Clara, CA). All samples had a RNA integrity number of 9.0 or higher. Samples containing 375 ng total RNA were amplified and labeled using the TotalPrep RNA amplification kit (Ambion, Austin, TX) following the standard kit protocols. The hybridization mix containing 750 ng of labeled-amplified RNA was prepared and loaded onto the Sentrix RatRef-12 Expression Beadchip (Illumina, San Diego, CA) using the supplied reagents, hybridized for 20 hours at 58°C in an Illumina Hybridization Oven, and washed and dried according to the Whole-Genome Gene Expression with IntelliHyb Seal System Manual (Illu-

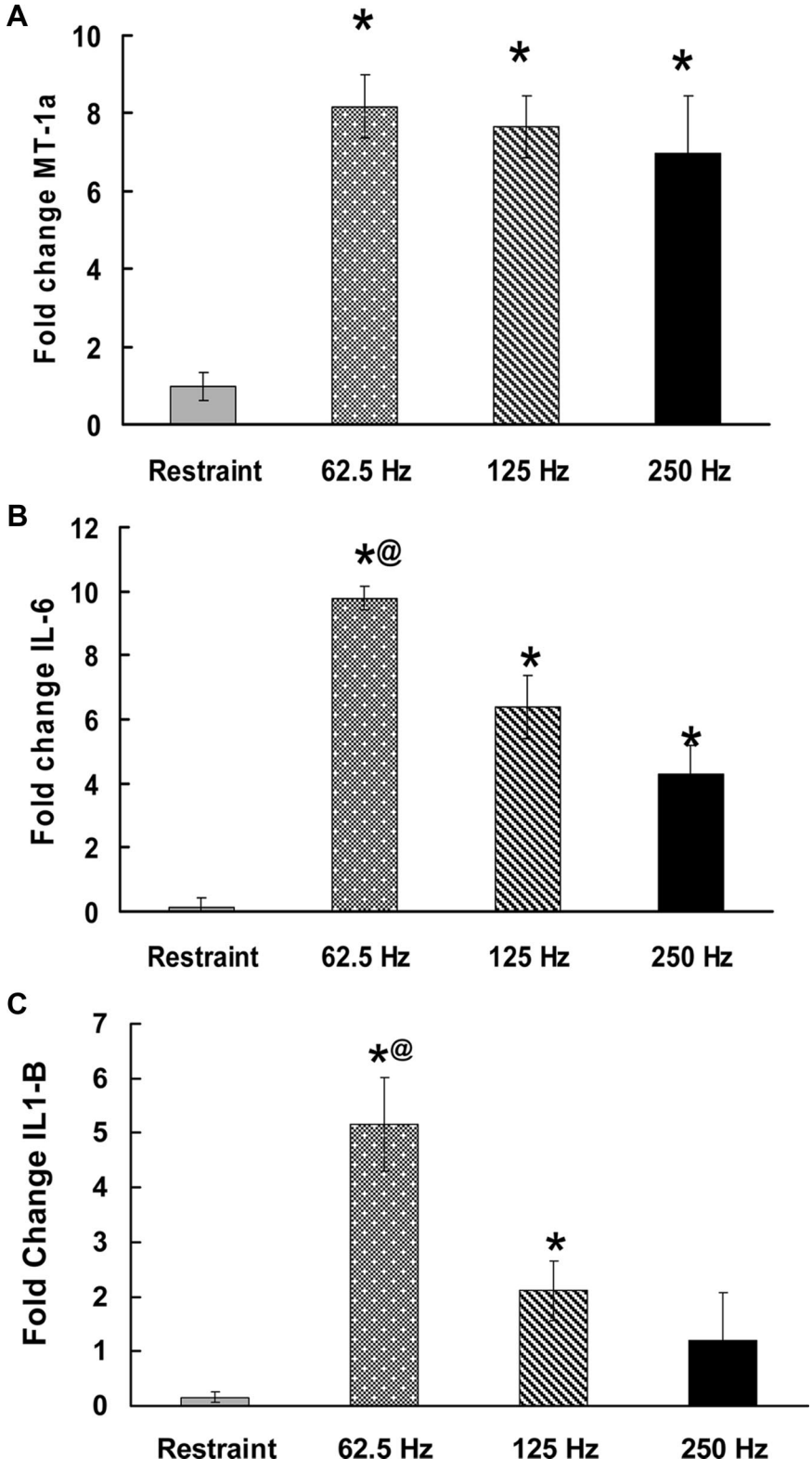

FIGURE 1. Gene expression measured by quantitative RT-PCR in the ventral tail artery (expressed as the mean fold change compared with cage-control ± SEM). Exposure to vibration generally resulted in an increase in MT1 (A) and IL-6 (B) expression in arteries (*Greater than restraint controls, $P < 0.05$). However, IL-6 expression (C) was significantly higher in arteries from rats exposed to vibration at 62.5 Hz than 125 or 250 Hz (@$P < 0.05$). IL-1β expression was highest in the arteries of rats exposed to vibration at 62.5 Hz. However, a smaller but significant increase was also seen in rats exposed to vibration at 125 Hz.

mina). Chips were taken to Allegheny Singer Research Institute (Pittsburgh, PA) for scanning.

Files containing fluorescent intensity from the bead scanner were loaded into Beadstudio (Framework version 3.0.19.0) Gene Expression module version 3.0.1.4. Housekeeping, hybridization control, stringency, and negative control genes were checked for proper quality control. Beadarray expression data were then exported with mean fluorescent intensity across like beads and bead variance estimates into flat files for subsequent analyses.

Quantitative RT-PCR

Quantitative real-time PCR (qRT-PCR) was performed to confirm vibration-induced changes in transcript levels seen using the arrays and to determine if vibration resulted in changes in the expression of inflammatory cytokines, apoptotic factors, or specific vasomodulating factors involved in vascular remodeling (see Table 2 and Fig. 1). Ribosomal 18s was used as a loading control. Transcripts examined and primer sequences are listed in Table 1. RNA isolated for the arrays was used, and first strand cDNA was synthesized from 1 μg of total RNA using Invitrogen's Reverse Transcription System (Invitrogen, Carlsbad, CA). Control RNA from heart tissue was run at 10× dilutions for each transcript to establish a standard curve of relative transcript levels, and relative RNA levels were calculated using this curve. Samples that did not show a single defined melt peak in the 80°C range were not included in the data set.

Immunohistochemistry

Cross-sections of the ventral tail artery (10 μm) were cut on a cryostat, thaw mounted onto charged slides, and stored at −20°C until used for IHC. Consecutive sections on a single slide were collected, so that they were ~100 μm apart. IHC was used to look for vibration-induced changes in the expression of nitrotyrosine, a marker of oxidative stress. We also performed IHC for the antioxidant, metallothionein (MT)-1, and the cytokines, interleukin (IL)-6 and IL-1β, because these factors increase in response to increases in oxidative activity in arteries, and they may play a role in vascular remodeling.[24–26] Primary antibodies used were nitrotyrosine (1:100 dilution, anti-mouse IgG; Santa Cruz), IL-1β (1:400 dilution, anti-rabbit; Abcam), MT-1 (1:185 dilution, anti-rabbit; Santa Cruz), and IL-6 (1:75 dilution, anti-goat; Santa Cruz). The secondary antibody was Cy3-labeled IgGs (used at 1:200 to 1:500; Jackson Immunolabs, West Grove, CA). All slides were stained with DAPI, coverslipped with Prolong Gold (Invitrogen), and digital images were taken using a Zeiss LSM510 laser scanning confocal microscope, with HeNe, Argon, and ultraviolet lasers, and integrated 2D and 3D image-processing software. Images were imported into Scion Image (Scion, Inc), and density thresholds and brightness were set and maintained for all tissue samples. The immunostained area that was above threshold was measured in each artery, and the average was calculated and used in the analyses.

Analyses

Fold changes in transcript levels, immunostained area of the arteries, and the morphological data (VSM thickness and lumen diameter) were analyzed using one-way ANOVAs. Differences with $P < 0.05$ were considered significant unless otherwise noted.

Illumina BeadArray expression data were analyzed in Bioconductor[27] using the "lumi" and "limma" packages. The lumi Bioconductor package was specifically developed to process Illumina microarrays and covers data input, quality control, variance stabilization, normalization, and gene annotation.[28] The back-

TABLE 1. Accession Numbers and Primer Sequences Used for Quantitative RT-PCR

Gene	Accession Number	Primer Sequences
α2A Adrenoreceptor	NM_012739	2A-F 5′-TGTGTTGGTTCCCGTTCTT-3′
		2A-R 5′-CGGAAGTCGTGGTTGAAAAT-3′
α2C Adrenoreceptor	NM_138506	2C-F 5′-GGGTTTCCTCATCGTTTTCA-3′
		2C-R 5′-GAAAAGGGCATGACCAGTGT-3′
Bax	NM_017059	BAX-F 5′-TGTTTGCTGATGGCAACTTC-3′
		BAX-R 5′-GATCAGCTCGGGCACTTTAG-3′
Bcl2	NM_016993	BCL-2-F 5′-GGGATGCCTTTGTGGAACTA-3′
		BCL-2- R 5′-CTCACTTGTGGCCCAGGTAT-3′
IL-1β	M98820	IL-1β-F 5′-CAGGAAGGCAGTGTCACTCA-3′
		IL-1β-R 5′-AAAGAAGGTGCTTGGGTCCT-3′
IL-6	NM_012589	IL-6-F 5′-CCGGAGAGGAGACTTCACAG-3′
		IL-6-R 5′-CAGAATTGCCATTGCACAAC-3′
Cox_2	S67722.1	COX-2-F 5′-ACCAACGCTGCCACAACT-3′
		COX-2-R 5′-GGTTGGAACAGCAAGGATTT-3′
ET-1	NM_012548	Eth-1-F 5′-ACTTCTGCCACCTGGACATC-3′
		Eth-1-R 5′-CTGTTCCCTTGGTCTGTGGT-3′
Mt1a	NM_138826.4	Mt1a-F 5′-CACCAGATCTCGGAATGGAC-3′
		Mt1a-R 5′-GCAGCAGCTCTTCTTGCAG-3′
NOS-3 (eNOS)	NM_021838	NOS-3-F 5′-TGACCCTCACCGATACAACA-3′
		NOS-3-R 5′-CTGTACAGCACAGCCACGTT-3′
NOS-2 (iNOS)	NM_012611	NOS-2-F 5′-CCTGTGTTCCACCAGGAGAT-3′
		NOS-2-R 5′-CGCTTTCACCAAGACTGTGA-3′
NPY	NM_012614.1	NPY-F 5′-CAAGCTCATTCCTCGCAGA-3′
		NpPY-R 5′-CATTCGTTTGTTACCTAGCATCA-3′
Runx	NM_017325.1	Runx1-F 5′-CCTCCTTGAACCACTCCACT-3′
		Runx1-R 5′-CTGGATCTGCCTGGCATC-3′
Timp-1	NM_053819.1	TIMP1-F 5′-CAGCAAAAGGCCTTCGTAAA-3′
		TIMP1-R 5′-TGGCTGAACAGGGAAACACT-3′
TNF-α	NM_012675	TNFα-F 5′-ATGTGGAACTGGCAGAGGAG-3′
		TNFα-R 5′-CAATCACCCCGAAGTTCAGT-3′

F, forward; R, reverse.

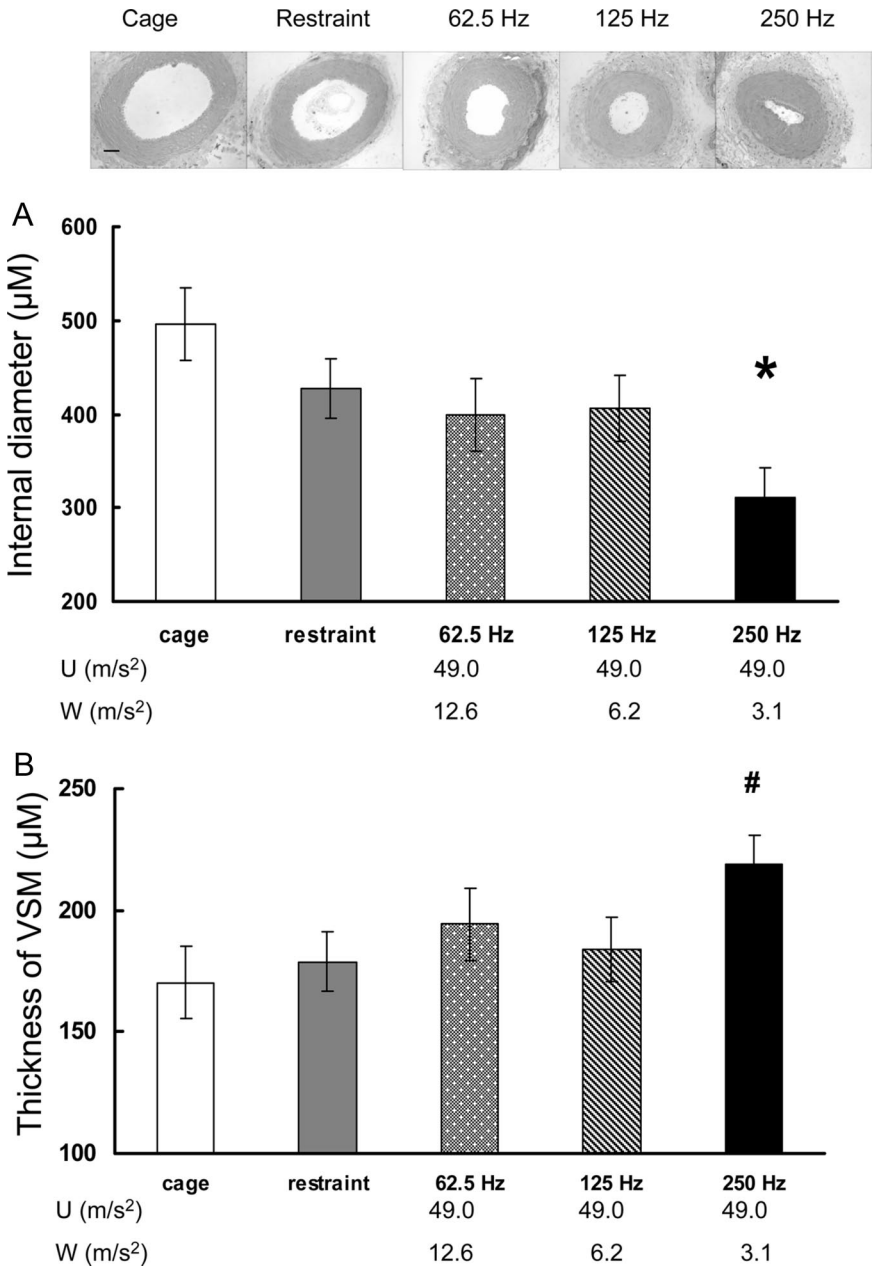

FIGURE 2. The photomicrographs display morphological changes in the ventral tail arteries of rats exposed to tail vibration for 10 days (bar = 50 μM). The *x* axis shows the exposure frequency and the unweighted (U) and ISO-weighted (W) accelerations. The luminal diameter was smaller in rats exposed to vibration at 250 Hz than in cage- or restraint-control rats (A; *Less than cage or restraint controls, $P < 0.05$). Vibration at 250 Hz also resulted in an increase in the thickness of the VSM (B; #Greater than cage control, $P < 0.05$). Data are expressed as group means ± SEM.

ground correction method was "force positive" and was used to force all expression values to be positive by adding an offset (minus minimum values plus 1). Data were then transformed using a variance-stabilizing transformation. The variance-stabilizing transformation method takes advantage of the technical replicates available on an Illumina microarray.[29] Data normalization then proceeded using the robust spline normalization algorithm, which combines the features of quantile and loess normalization.[29] Before subsequent analyses including differential expression analysis, unexpressed genes are filtered out.

Normalized data were then analyzed using the limma package in Bioconductor.[30] Limma was used to fit a linear model for each gene and generate group means of expression values, *P*-values, and fold changes between groups. These lists of genes and their associated statistics were used as input for subsequent bioinformatic analyses using Ingenuity Pathways Analysis (Ingenuity® Systems, www.ingenuity.com).

RESULTS

Morphology

Exposure to vibration affected the luminal diameter of ventral-tail arteries (Fig. 2, $F_{(4, 20)} = 3.71$, $P < 0.03$). Reductions in lumen diameter (compared with cage controls) were as follows: restraint control, −12.94%; 62.5 Hz, −15.21%; −125 Hz, −14.41%; and 250 Hz, −35.14%. Nevertheless, only rats exposed to vibration at 250 Hz showed a significant reduction in diameter when compared with cage and restraint controls ($P < 0.05$). Vibration also resulted in an increase in VSM thickness. Changes in thickness compared with cage controls were as follows: restraint control +5%; 62.5 Hz, +14%; 125 Hz, +8%; and 250 Hz, +28%. However, as with lumen diameter, only arteries from rats exposed to vibration at 250 Hz displayed significant increases in VSM thickness when compared with cage and restraint controls ($P < 0.05$). Vibration did not result in a significant change in the

overall diameter of the arteries (mean μm ± SEM; cage control, 649 ± 37.14; restraint control, 654.89 ± 30.32; 62.5 Hz, 646.85 ± 37.14; 125 Hz, 640.37 ± 33.22; and 250 Hz, 590.12 ± 30.32).

Gene Arrays

Analyses comparing transcript levels between cage- and restraint-control rats did not reveal any significant differences between these two groups (using a fold change of 1.5 and $P < 0.01$ as significant). Using the same fold change and significance values, the transcript levels in restraint-control arteries were compared with those in vibrated arteries, and the recognized transcripts showing significant changes are presented in Table 2. Using these data, pathways were generated to determine which cellular processes were affected by vibration and may underlie vibration-induced changes in vascular function. Two interacting pathways were identified, one involved in lipid metabolism and another involved in cell signaling, cancer, cell development, and cell morphology.

TABLE 2. Gene Expression in Ventral Tail Arteries of Vibrated Rats

	Fold Change From Restraint (*P*)		
Gene	**63 Hz**	**125 Hz**	**250 Hz**
Ca3			
Carbonic anhydrase III			−3.08 (0.009)
Cdo1			
Cysteine dioxygenase, type I			−2.48 (0.002)
Ces1			
Carboxylesterase 1			−3.84 (9E − 4)
Cidec			
Cell-death inducing DFFA-like effector c			−1.56 (0.002)
Cyp26b1			
Cytochrome P450, family 26 subfamily B, polypeptide 1		−1.56 (0.001)	−1.64 (4E − 4)
Dgat2			
Diacylglycerol *O*-acyltransferase 2			−2.15 (0.002)
Errfi1			
ERB-B receptor feedback inhibitor-1			−1.74 (0.002)
JunB			
Jun B protoncogene	1.97 (0.002)		
Mgst1			
Microsomal glutathione S-transferase 1			−3.20 (0.006)
Mgst2			
Microsomal glutathione S-transferase 1			−1.83 (0.005)
Mt1a			
Metallothionein 1a	3.87 (6.3E − 5)	3.68 (9.7E − 5)	3.15 (3.7E − 4)
Npy			
Neuropeptide Y		−1.57 (0.002)	−1.63 (0.001)
carboxykinase 1 (soluble)		−1.54 (0.008)	−2.06 (0.003)
Per1			
Period homolog 1 (drosophila)	−1.55 (0.004)	−1.75 (5.7E − 4)	−1.76 (5.5E − 4)
Rasd1 1.71 (4.3E-4)			
RAS, dexamethasone-induced 1			−1.67 (0.003)
Runx1			
Runt-related transcription Factor 1	1.77 (0.006)	1.84 (0.003)	2.03 (0.001)
Thrsp			
Thyroid hormone responsive (SPOT14)			−6.01 (0.002)
Timp1			
Tissue inhibitor of metallopeptidase 1			1.55 (0.004)
Tmem49			
Transmembrane protein 49	1.53 (0.001)	1.54 (0.001)	1.53 (0.001)
Uap1			
UDP, *N*-acetylglucosamine pyrophosphorylase	2.11 (0.005)	1.89 (0.002)	1.73 (0.009)
Ugcg			
UDP-glucose ceramide glucosyltransferase	1.65 (0.004)		1.55 (0.009)

The data in this table are transcripts that showed changes in expression in response to vibration. Changes in expression levels were considered significant if the change from restraint control was 1.5-fold or greater, and the *P* value was <0.01. Transcripts that displayed changes in expression in response to vibration at all three frequencies are highlighted.

Quatitative PCR

We measured expression levels for some of the transcripts identified by the arrays (eg, MT1a, Runx, and Timp) and for inflammatory factors (eg, IL-6 and IL-1β), which may also play a role in vascular remodeling and injury. Figure 1 shows fold changes in transcript levels for Mt-1a, IL-6, and IL-1β. Mt-1a and IL-6 transcript levels were greater in arteries from vibrated rats than cage- or restraint-control rats ($P < 0.05$). IL-6 expression also was significantly greater in arteries from rats exposed to 62.5 Hz than in rats exposed to 125- or 250-Hz vibration. Other transcripts that were generally increased in tail arteries in response to vibration included the transcription factor Runx, tissue inhibitor of metalloproteinase (Timp)-1, and α2A-adrenoreceptor (Table 3).

The expression of IL-1β was higher in rats exposed to vibration at 62.5 and 125 Hz than in rats from either control group ($P < 0.05$). IL-1β expression was also higher in arteries from rats exposed to 62.5 Hz than rats exposed to the other two vibration frequencies ($P < 0.05$). Nos-3 and endothelin-1 expression levels also tended to be highest in rats exposed to vibration at 62.5 Hz.

Immunohistochemistry

Nitrotyrosine was used as a marker of oxidative stress in this study. Analyses of the immunostained areas demonstrated that there was an effect of vibration on the nitrotyrosine staining in ventral arteries (Fig. 3, $F_{(4,29)} = 4.10$, $P = 0.009$). Nitrotyrosine staining in arteries from rats exposed to vibration at 125 Hz was greater than the staining in cage-control rats ($P < 0.05$), and arteries from rats exposed to vibration at 250 Hz had more staining than arteries from cage-controls, restraint-controls, or rats exposed to vibration at 62.5 Hz ($P < 0.05$). Although there appears to be differences in the luminal and total diameter of these arteries, these differences are not reliable because artery segments used for IHC were not fixed before being dissected from the tail. Thus, changes in size and shape are most likely the result of handling. Because qRT-PCR results demonstrated that IL-6, IL-1β, and MT-1a also were affected by vibration, we performed IHC to determine if we could detect vibration-induced changes in staining for any of these factors. Vibration did not affect the area stained with IL-1β (Fig. 4). However, pairwise comparisons demonstrated that MT-1 immunolabeling was greater in arteries from rats exposed to vibration at 250 Hz than restraint-control rats ($P < 0.05$). There was not a significant affect of treatment on IL-6 staining ($F_{(4,28)} = 2.59$, $P = 0.058$), but planned pairwise comparisons performed to determine if vibrated rats were different than control rats revealed that the immunostained area in arteries from cage- and restraint-control rats was less than the stained area in arteries from rats exposed to vibration at 250 Hz ($P < 0.02$).

DISCUSSION

ISO standard 5349-1 and ANSI standard 2.70 use frequency weighting to estimate the risk of injury associated with exposure to hand-transmitted vibration. Greater weighting is given to lower frequency (ie, $\leq$32 Hz) vibrations, indicating that exposure to these frequencies poses a greater risk of inducing an injury. However, recent epidemiologic and experimental studies suggest that this frequency weighting may underestimate the risk of injury associated with exposure to higher frequency vibrations (eg, >100 Hz). Modeling and experimental studies have demonstrated that exposure to higher vibration frequencies induces more stress and strain on soft tissues and this increased stress/strain could actually increase the risk of injury. On the basis of these studies, we hypothesized that the risk of developing vibration-induced vascular dysfunction would be increased with exposures to frequencies that induce the greatest stress and strain on exposed tissues.[9,11,22] The findings of this study are consistent with this hypothesis; although vibration exposures at all frequencies resulted in cellular, molecular, and morphological changes that could lead to prolonged vascular dysfunction in the ventral tail arteries of rats, these changes were most pronounced in arteries from rats exposed to vibration at 250 Hz, the frequency that induces the most stress on soft tissues.

Vibration-induced vascular changes in this study were assessed by examining the effects of vibration on morphology, inflammation, and oxidative stress. We found that vibration exposure resulted in morphological changes indicative of vascular remodeling; the luminal diameters were generally reduced, and the VSM thickness was increased in arteries from vibration-exposed rats. Nevertheless, these changes were only significant in rats exposed to vibration at 250 Hz and not in rats exposed to 62.5 or 125 Hz. These findings are consistent with those of a previous study demonstrating that vibration induces remodeling in rat hind limb arteries after 90 days, but not 30 days of vibration exposure at 60 Hz and 5 g.[31] Vascular remodeling often occurs as a response to changes in stress across the muscle wall because of increases in the

TABLE 3. Transcript Levels in Ventral Tail Arteries From Control and Vibrated Rats After 10 d of Exposure

Gene	Restraint Control	62.5 Hz	125 Hz	250 Hz
α2A Adrenoreceptor	−0.24 ± 0.10	2.91 ± 0.53*	1.85 ± 0.66	2.07 ± 0.35*
α2C Adrenoreceptor	−0.23 ± 0.13	0.73 ± 0.08	0.04 ± 0.09	1.05 ± 0.70
Bax	−0.64 ± 0.07	1.33 ± 0.54	0.86 ± 0.08	1.05 ± 0.32
Bcl2	−0.49 ± 0.06	−0.27 ± 0.05	−0.76 ± 0.04	0.45 ± 0.09
Cox_2	0.84 ± 0.08	1.37 ± 0.16	0.86 ± 0.05	−0.11 ± 0.08
ET-1	0.06 ± 0.26	3.33 ± 0.31†	1.45 ± 0.65	0.54 ± 0.05
Nos-3	−0.19 ± 0.06	3.09 ± 0.59*	1.79 ± 0.09	1.14 ± 0.53
Nos-2	−0.32 ± 0.07	0.43 ± 0.04	−0.17 ± 0.06	0.52 ± 0.09
Npy	1.46 ± 0.52	1.27 ± 0.36	0.34 ± 0.08	0.50 ± 0.10
Runx	−0.56 ± 0.03	4.03 ± 0.45*	3.21 ± 0.52*	4.39 ± 0.48*
Timp-1	0.08 ± 0.03	2.12 ± 0.26*	1.73 ± 0.15*	2.56 ± 0.30*
Tnf-α	−0.66 ± 0.12	1.87 ± 0.47	1.23 ± 0.05	2.15 ± 0.87

The data are presented as the fold change from cage control ± SEM ($n = 4$ rats/group).
*Greater than cage- and restraint-control, $P < 0.05$.
†Greater than 250 Hz, $P < 0.05$.

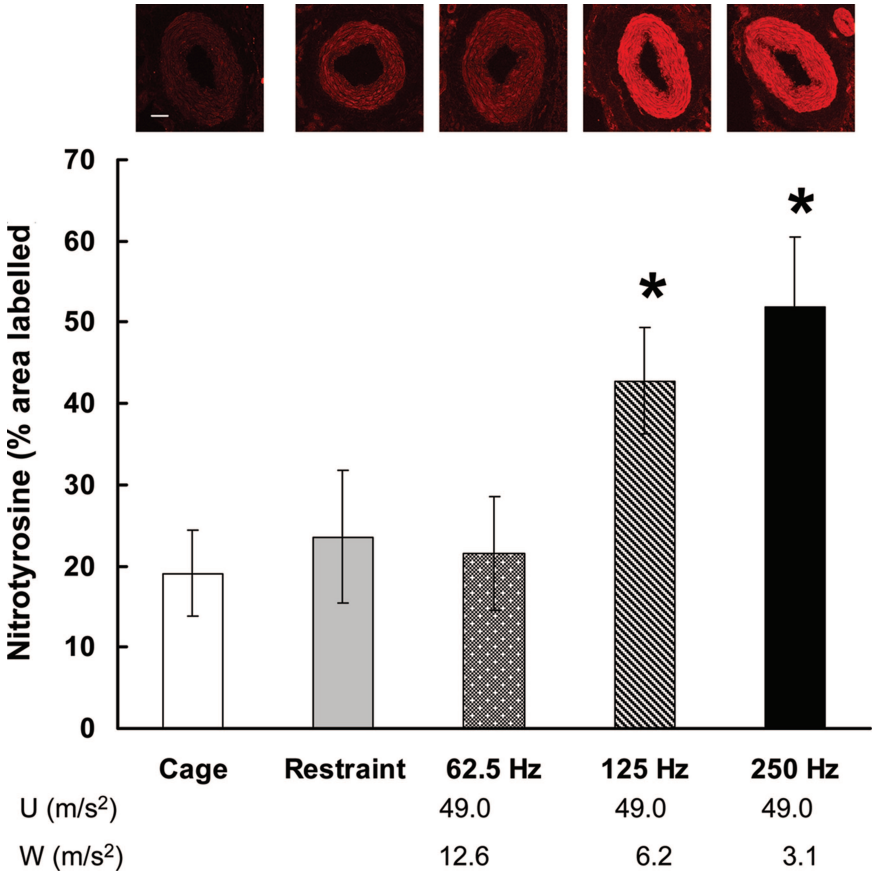

FIGURE 3. The photomicrographs show nitrotyrosine staining in arteries from rats exposed to control and vibration conditions (bar = 50 μM). The *x* axis shows the exposure frequency and the unweighted (U) and ISO-weighted (W) accelerations. Analyses of the immunostained area (mean ± SEM) within arteries demonstrated that staining was significantly higher in arteries of rats exposed to vibration at 125 or 250 Hz than in arteries of rats from the other three conditions (*$P < 0.05$).

internal pressure, reductions in the internal diameter of the vessel, or both.[32–34] Remodeling is also associated with vascular dysfunction in a number of diseases including HAVS, diabetes, and hypertension.[33,35] Because vibration results in vasoconstriction of cutaneous blood vessels[12,36,37]and external stress on strain on the artery wall,[11] it is not surprising that remodeling was seen in arteries collected from rats exposed to vibration. What was interesting was that vascular remodeling seemed to be more prominent as the frequency of the vibration exposure increased. This may be because the vibration-induced stress and strain on the vessel also increases as the vibration frequency increases between 62.5 and 250 Hz.[11,15] Although we have not measured the actual stress and strain on blood vessels or any other soft tissues, the results of modeling studies suggest that the local soft tissue absorbs virtually all of the vibration energy at frequencies greater than 100 Hz.[11,15]

Vibration may cause stress and strain on the artery directly or by inducing the constriction of peripheral blood vessels, which in turn increases flow-mediated shear stress. Vibration can enhance peripheral vasoconstriction by inducing hyperactivity of the sympathetic nervous system. For example, 24 hours urinary excretion of norepinephrine (NE) was generally increased in workers with HAVS,[38] and increases in plasma NE concentrations in response to cold were also greater in workers with HAVS than controls.[39] In addition, workers with HAVS display a greater increase in urinary NE concentrations in response to psychologic stressors than controls.[40] We did not directly assess vibration-induced changes in sympathetic activity in this study. However, analyses of the gene array data demonstrates that transcripts involved in lipid metabolism were affected by vibration, and sympathetic activity plays a major role in regulating lipid metabolism (Table 2).[41,42] Vibration may have also resulted in other systemic responses that led to changes in lipid metabolism. Additional studies need to be performed to determine the exact contribution of systemic changes to vibration-induced vascular dysfunction.

Vibration can also act locally to reduce blood flow by increasing vascular responsiveness to α2-adrenoreceptor-mediated vasoconstriction.[6] Although we did not assess vascular responsiveness to adrenoreceptor-mediated constriction in this study, we have demonstrated α2C-adrenoreceptor-mediated vasoconstriction is enhanced after 1 and 10 days of exposure to vibration at 125 Hz.[12,14] Because prolonged vasoconstriction can induce vascular remodeling,[32,43] an increase in sympathetic activity, and an increased sensitivity of the peripheral vasculature to NE-induced vasoconstriction, these factors may have interacted to contribute to the inward remodeling seen in this experiment and may contribute to the long-term vascular dysfunction seen in workers with VWF.[44]

A number of other factors also may have contributed to the vascular remodeling seen in arteries from rats exposed to vibration. One possibility is that the vibration-induced increases in oxidative activity and inflammation stimulated remodeling of the ventral tail arteries. Vibration exposure, particularly at the higher frequencies, resulted in an increase in nitrotyrosine staining in arteries. Nitrotyrosine has been used as a marker of protein nitration and oxidative damage in tissues.[45] The findings of this study are consistent with other results from our laboratory demonstrating that vascular hydrogen peroxide concentrations are increased after 10 days of exposure to vibration at 125 Hz.[14] The vibration-induced increase in *MT-1a* gene expression and MT-1 protein levels are also indicative of an increase in oxidative activity.[46,47] Although MT-1a transcript expression was increased in response to vibration at all frequencies in this study, immunostaining for MT-1 tended to be higher only in rats exposed to vibration at 250 Hz. Vibration also

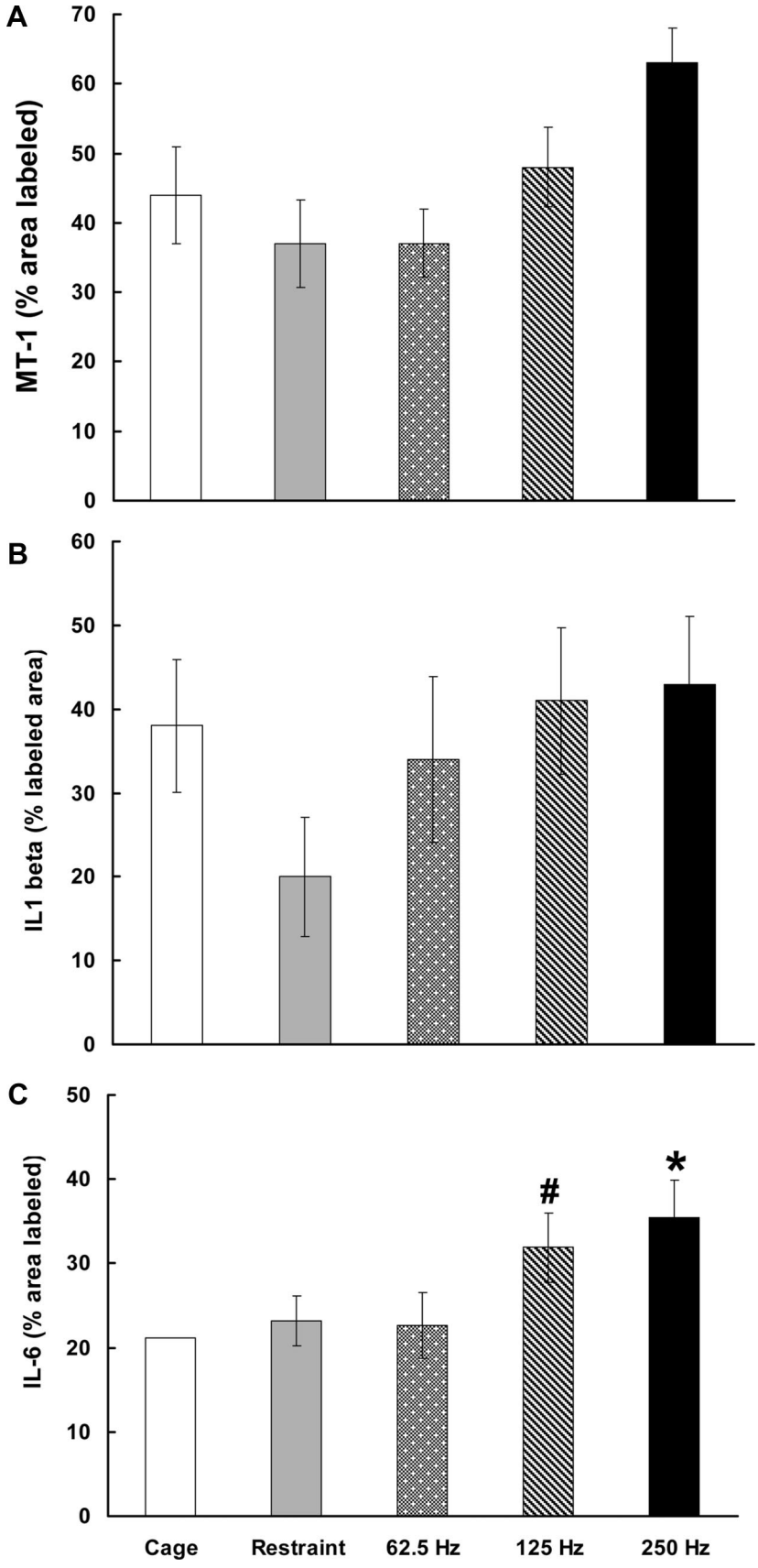

FIGURE 4. Immunostaining for MT-1, IL-1β, and IL-6 in ventral tail arteries of rats exposed to vibration. Although vibration exposure appeared to result in a slight increase the areas of arteries immunostained for MT-1 (A) and IL-1β (B), these differences were not significant. However, vibration did result in an increase in IL-6 (C) staining in arteries, with IL-6 being higher in arteries from rats exposed to vibration at 125 and 250 Hz than in arteries from control rats (#Greater than cage-controls, $P < 0.05$; *Greater than cage and restraint control, $P < 0.05$).

resulted in an increased expression of the cytokines, IL-1β, and IL-6 in ventral tail arteries, with transcript levels being highest in rats exposed to vibration at 62.5 Hz. We hypothesize that transcript levels for these cytokines may have been increased with exposure to higher frequencies at an earlier time point, but additional studies examining the time course of cytokine induction will need to be performed. Nevertheless, when we examined protein levels, we found that immunolabeling for IL-1β was not affected by vibration and IL-6 labeling was increased in arteries after exposure to vibration at 125 or 250 Hz, suggesting that IL-6 protein levels were higher at these frequencies. Increases in a number of cytokines, including IL-6, IL-1β, and TNF-α, have all been linked to vascular dysfunction, disease and remodeling.[48,49]

The results of these studies demonstrate that exposure to vibration at frequencies above 100 Hz can induce changes that may lead to vascular dysfunction. In fact, it appears that vibration may induce remodeling, oxidative activity, and inflammation more quickly at higher frequencies. In this study, rats were exposed to vibration for 4 hr/d. Using the weighted acceleration to determine risk of injury would suggest that rats exposed to vibration at 62.5 Hz (weighted frequency of 12.6 m/s^2) would display the greatest level of vascular disruption and exposures to vibration at 125 and 250 Hz (weighted accelerations of 6.2 and 3.1 m/s^2, respectively) for 4 hours should have no or minimal effects. Nevertheless, the opposite effects were seen; markers of dysfunction and remodeling were less pronounced at 62.5 Hz than at 250 Hz. This is most likely because soft-tissue stress and strain is greater at frequencies between 100 and 300 Hz than at lower frequencies[11] and suggests that the current weighting in the ISO-5349 standard may not accurately represent the frequency-dependent effects of vibration.

It is reasonable to assume that frequency-dependent vascular responses to vibration seen in our model are similar to the changes seen in human fingers because the frequency-dependent responses of the soft-tissues of the fingers and of the rat tail are similar, particularly at frequencies above 100 Hz. These data also suggest that ISO-5349 may overestimate the risk of vascular injury associated with exposure to lower frequency vibration but underestimate the risk of injury caused by exposure to higher frequencies. These data also are consistent with recent modeling, experimental, and epidemiological studies in humans suggesting that exposure to vibration frequencies above 100 Hz is capable of inducing vascular dysfunction[50–52] and provide additional support for revising the ISO-5349 weighting curve, so that greater emphasis is given to exposures to higher frequency vibrations.

ACKNOWLEDGMENT

This research was funded by the Health Effects Laboratory Division at the National Institute for Occupational Safety and Health.

REFERENCES

1. Bernard BP. *Hand-Arm Vibration Syndrome. Musculoskeletal Disorders and Workplace Factors. A Critical Review of Epidemiological Evidence for Work-Related Musculoskeletal Disorders of the Neck, Upper Extremity, and Low Back.* Cincinnati, OH: US Department of Health and Human Services, National Institute for Occupational Safety and Health; 1997:5c-1–5c-31.
2. Stoyneva Z, Lyapina M, Tzvetkov D, Vodenicharov E. Current pathophysiological views on vibration-induced Raynaud's phenomenon. *Cardiovasc Res*. 2003;57:615–624.
3. Takeuchi T, Futatsuka M, Imanishi H, Yamada S. Pathological changes observed in the finger biopsy of patients with vibration-induced white finger. *Scand J Work Environ Health*. 1986;12:280–283.
4. Dowd PM, Goldsmith PC, Chopra S, Bull HA, Foreman JC. Cutaneous responses to endothelin-1 and histamine in patients with vibration white finger. *J Invest Dermatol*. 1998;110:127–131.
5. Kennedy G, Khan F, McLaren M, Belch JJ. Endothelial activation and response in patients with hand arm vibration syndrome. *Eur J Clin Invest*. 1999;29:577–581.
6. Lindblad LE, Ekenvall L. Alpha 2-adrenoceptor inhibition in patients with vibration white fingers. *Kurume Med J*. 1990;37(suppl):S95–S99.
7. Dong RG, Welcome DE, McDowell TW, Wu JZ. Biodynamic response of human fingers in a power grip subjected to a random vibration. *J Biomech Eng*. 2004;126:447–457.
8. Burstrom L, Lundstrom R. Absorption of vibration energy in the human hand and arm. *Ergonomics*. 1994;37:879–890.
9. Dong RG, Schopper AW, McDowell TW, et al. Vibration energy absorption (VEA) in human fingers-hand-arm system. *Med Eng Phy*. 2004;26:483–492.
10. Wu JZ, Welcome DE, Dong RG. Three-dimensional finite element simulations of the mechanical response of the fingertip to static and dynamic compressions. *Comput Methods Biomech Biomed Engin*. 2006;9:55–63.
11. Wu JZ, Welcome DE, Krajnak K, Dong RG. Finite element analysis of the penetrations of shear and normal vibrations into the soft tissues in a fingertip. *Med Eng Physics*. 2007;29:718–727.
12. Krajnak K, Dong RG, Flavahan S, Welcome DE, Flavahan NA. Acute vibration increases a_{2c}-adrenergic smooth muscle constriction and alters thermosensitivity of cutaneous arteries. *J Appl Physiol*. 2006;100:1230–1237.
13. Krajnak K, Waugh S, Wirth O, Kashon ML. Acute vibration reduces Aβ nerve fiber sensitivity and alters gene expression in the ventral tail nerves of rats. *Muscle Nerve*. 2007;36:197–205.
14. Krajnak K, Waugh S, Johnson C, Miller R, Kiedrowski M. Vibration disrupts vascular function in a model of metabolic syndrome. *Ind Health*. 2009;47:533–542.
15. Welcome DE, Krajnak K, Kashon ML, Dong RG. An investigation on the biodyamic foundation of a rat tail model. *Proc Inst Mech Eng H*. 2008;222:1127–1141.
16. Govindaraju SR, Curry BD, Bain JL, Riley DA. Comparison of continuous and intermittent vibration effects on rat-tail artery and nerve. *Muscle Nerve*. 2006;34:197–204.
17. Hughes JM, Wirth O, Krajnak K, et al. Increased oxidant activity mediates vascular dysfunction in vibration injury. *J Pharmacol Exp Ther*. 2009;328:223–230.
18. Langille BL. Arterial remodeling: relation to hemodynamics. *Can J Physiol Pharmacol*. 1996;74:834–841.
19. Saski N, Yamashita T, Takaya T, et al. Augmentation of vascular remodeling by uncoupled endothelial nitric oxide synthase in a mouse model of diabetes mellitus. *Arterioscler Thromb Vasc Biol*. 2008;28:1068–1076.
20. Albelda SM, Smith CW, Ward PA. Adhesion molecules and inflammatory injury. *FASEB J*. 1994;8:504–512.
21. Dyck PJ, Giannini C. Pathologic alterations in the diabetic neuropathies of humans: a review. *J Neuropath Exp Neurol*. 1996;55:1181–1193.
22. Bovenzi M, Lindsell CJ, Griffin MJ. Acute vascular responses to the frequency of vibration transmitted to the hand. *Occup Environ Med*. 2000;57:422–430.
23. Curry BD, Govindaraju SR, Bain JL, et al. Evidence for frequency-dependent arterial damage in vibrated rat tails. *Anat Rec A Discov Mol Cell Evol Biol*. 2005;284:511–521.
24. Pitt BR, Schwarz M, Woo ES, et al. Overexpression of metallothionein decreases sensitivity of pulmonary endothelial cells to oxidant injury. *Am J Physiol*. 1997;273:L856–L865.
25. Dagues N, Pawlowski V, Guigon G, et al. Altered gene expression in rat mesenteric tissue following in vivo exposure to a phosphodiesterase 4 inhibitor. *Toxicol Appl Pharmacol*. 2007;218:52–63.
26. Wohlin M, Helmersson J, Sundstrom J, et al. Both cyclooxygenase- and cytokine-mediated inflammation are associated with carotid intima-media thickness. *Cytokine*. 2007;38:130–136.
27. Gentleman RC, Carey VJ, Bates DM, et al. Bioconductor: open software development for computational biology and bioinformatics. *Genome Biol*. 2004;5:R80.
28. Du P, Kibbe WA, Lin SM. Lumi: a pipeline for processing Illumina microarray. *Bioinformatics (Oxford, England)*. 2008;24:1547–1548.
29. Lin SM, Du P, Huber W, Kibbe WA. Model-based variance-stabilizing transformation for Illumina microarray data. *Nucleic Acids Res*. 2008;36:e11.
30. Smyth GK. Linear models and empirical Bayes methods for assessing differential expression in microarray experiments. *Statistical Applications in Genetics and Molecular Biology*. 2004;3:Article 3.
31. Okada A, Inaba R, Furuno T. Occurrence of intimal thickening of the peripheral arteries in response to local vibration. *Br J Ind Med*. 1987;44:470–475.
32. Jacobsen JC, Mulvany MJ, Holstein-Rathlou NH. A mechanism for arterio-

lar remodeling based on maintenance of smooth muscle cell activation. *Am J Physiol Regul Integr Comp Physiol*. 2008;294:R1379–R1389.

33. Korshunov VA, Schwartz SM, Berk BC. Vascular remodeling: hemodynamic and biochemical mechanisms underlying Glagov's phenomenon. *Arterioscler Thromb Vasc Biol*. 2007;27:1722–1728.
34. Bakker ENTP, Pistea A, Spaan JAE, et al. Flow-dependent remodeling of small arteries in mice deficient for tissue-type transglutaminase: Possible compensation by macrophage-derived factor XIII. *Circ Res*. 2006;99:86–92.
35. Rizzoni D, Rosei EA. Small artery remodeling in diabetes mellitus. *Nutr Metab Cardiovasc Dis.* 2009;19:587–592.
36. Curry BD, Bain JL, Yan JG, et al. Vibration injury damages arterial endothelial cells. *Muscle Nerve*. 2002;25:527–534.
37. Bovenzi M, Welsh AJ, Griffin MJ. Acute effects of continuous and intermittent vibration on finger circulation. *Int Arch Occup Environ Health*. 2004;77:255–263.
38. Une H, Esaki H. Urinary excretion of adrenaline and noradrenaline in lumberjacks with vibration syndrome. *Br J Ind Med*. 1988;45:570–571.
39. Harada N. Autonomic nervous function of hand-arm vibration syndrome patients. *Nagoya J Med Sci.* 1994;57(suppl):77–85.
40. Harada N, Iwamoto M, Hirosawa I, et al. Response to psychological stressors in hand-arm vibration syndrome patients. *Cent Eur J Public Health.* 1995;3(suppl):54–56.
41. Seematter G, Binnert C, Tappy L. Stress and metabolism. *Metab Synd Rel Disorders*. 2005;3:8–13.
42. Bogaert YE, Linas S. The role of obesity in the pathogenesis of hypertension. *Nature Clin Prac*. 2009;5:101–111.
43. Price RJ, Skalak TC. Circumferential wall stress as a mechanism for arteriolar rarefaction and proliferation in a network model. *Microvasc Res*. 1994;47:188–202.
44. Ekenvall L, Lindblad LE. Is vibration white finger a primary sympathetic nerve injury? *Br J Ind Med*. 1986;43:702–706.
45. Beckman JS, Koppenol WH. Nitric oxide, superoxide and peroxynitrite: the good, the bad and the ugly. *Am J Physiol*. 1996;271:C1424–C1437.
46. Cai L. Diabetic cardiomyopathy and its prevention by metallothionein: experimental evidence, possible mechanisms and clinical implications. *Curr Medic Chem*. 2007;14:2193–2203.
47. Raleigh JA, Chou SC, Tables L, Suchindran S, Varia MA, Horsman MR. Relationship of hypoxia to metallothionein expression in murine tumors. *Int J Radiat Oncol Biol Phys*. 1998;42:727–730.
48. Chen LM, Liu B, Zhao HB, Stone P, Chen Q, Chamley L. IL-6, TNFalpha and TGFbeta promote nonapoptotic trophoblast deportation and subsequently causes endothelial cell activation. *Placenta.* 2010;31:75–80.
49. Fan Y, Ye J, Shen F, et al. Interleukin-6 stimulates circulating blood-derived endothelial progenitor cell angiogenesis in vitro. *J Cereb Blood Flow Metab*. 2008;28:90–98.
50. Wu JZ, Dong RG, Welcome DE. Biomechanics of humans hand-arm system in vibration: experimental and theoretical analysis. *Recent Res Devel Biomech*. 2009;3:43–84.
51. Dong RG, Dong JH, Wu JZ, Rakheja S. Modeling of biodynamic responses distributed at the fingers and the palm of the human hand-arm system. *J Biomech*. 2007;40:2335–2340.
52. Bovenzi M. Health risks from occupational exposures to mechanical vibration. *Med Lav*. 2006;97:535–541.